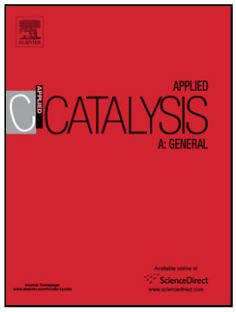

Title: Tailoring Sn-SBA-15 properties for catalytic isomerization of glucose

Authors: Juliana P. Lorenti, Eduardo Scolari, Elise M. Albuquerque, Marco A. Fraga, Jean Marcel R. Gallo

PII: S0926-860X(19)30203-0
DOI: https://doi.org/10.1016/j.apcata.2019.05.009
Reference: APCATA 17075

To appear in: *Applied Catalysis A: General*

Received date: 8 March 2019
Revised date: 2 May 2019
Accepted date: 6 May 2019

Please cite this article as: Lorenti JP, Scolari E, Albuquerque EM, Fraga MA, Gallo JMR, Tailoring Sn-SBA-15 properties for catalytic isomerization of glucose, *Applied Catalysis A, General* (2019), https://doi.org/10.1016/j.apcata.2019.05.009

Tailoring Sn-SBA-15 properties for catalytic isomerization of glucose

Juliana P. Lorenti,[a] Eduardo Scolari,[a] Elise M. Albuquerque,[b] Marco A. Fraga,[b] Jean Marcel R. Gallo[a,*]

[a]**G**roup of **Re**newable **E**nergy, **N**anotechnology, and **Cat**alysis (GreenCat), www.greencat.ufscar.br, Department of Chemistry, Federal University of São Carlos, Rod. Washington Luis, KM 235, CEP 13565-905, PO Box 676, São Carlos-SP, Brazil.
[b]National Institute of Technology/MCTIC, Division of Catalysis and Chemical Processes, Av. Venezuela, 82/518, CEP: 20081-312, Rio de Janeiro-RJ, Brazil.

*jean@ufscar.br

Graphical abstract

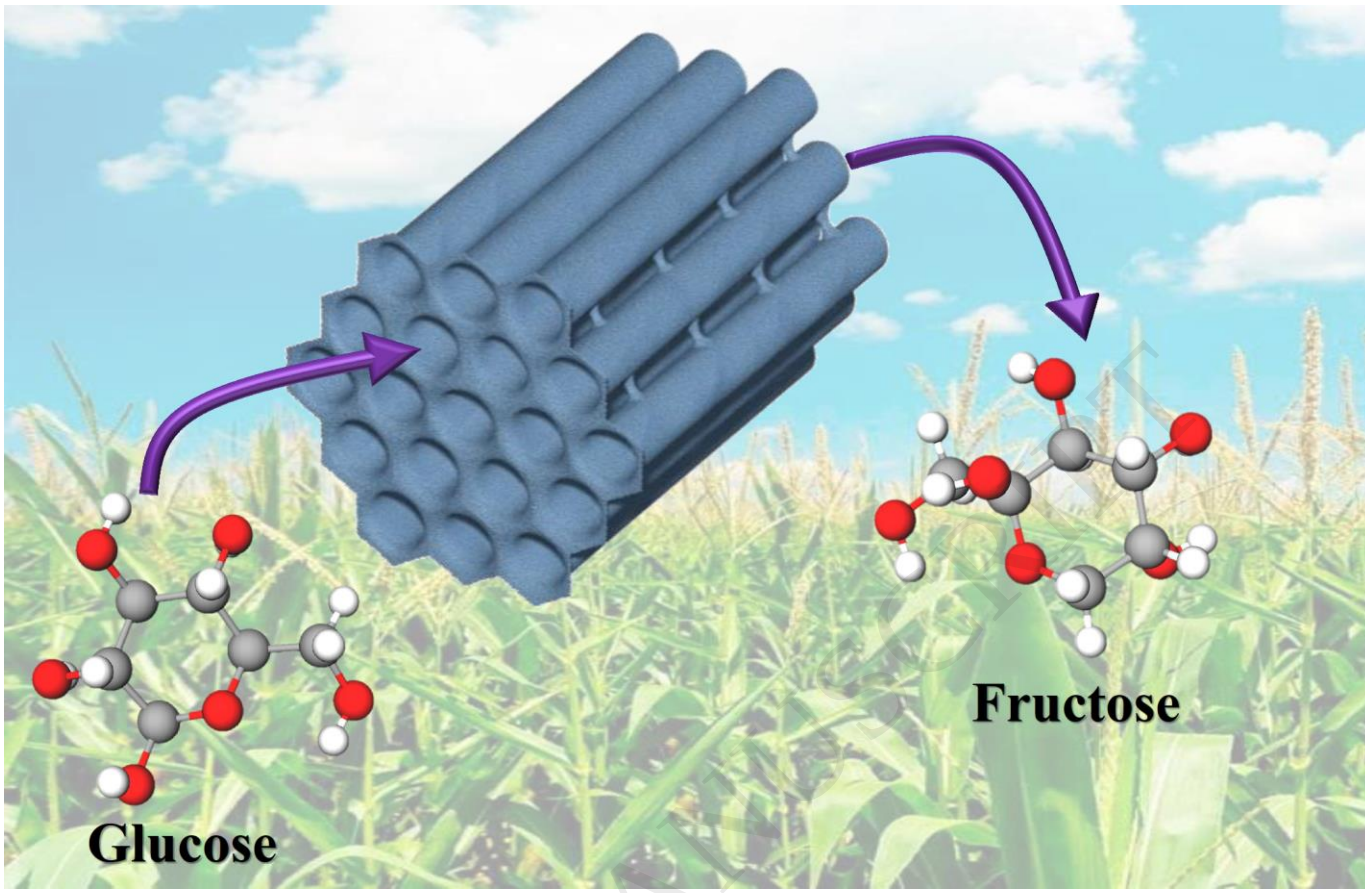

Highlights

- The synthesis pH and Sn loading affect the structural, textural, and catalytic properties of SBA-15.
- Catalysts with broad size distribution presented low TOF for fructose formation.
- Sample containing extra framework SnO2 reached the lowest TOF for fructose.
- TOF for fructose formation is affected by the solvent and increased as methanol<THF<GVL.

Abstract

Sn-SBA-15 was prepared by different methods seeking to tailor its catalytic properties. The effect of the SBA-15 synthesis pH and Sn loading in the Sn-SBA-15 structure, porosity, and type of generated Sn species on catalyst activity towards glucose isomerization was systematically evaluated. Increasing the acid concentration and the Sn loading led to a bimodal distribution of the unit cell parameter. Surface area, pore volume, and microporosity formation was not significantly affected by the synthesis parameter, while

the distribution of the large mesopores was. Indeed, the catalysts with broad size distribution presented lower TON for fructose formation compared to the ones with narrow distribution. The catalytic activity was also shown to be dependent on the nature of the solvent, and initial TOF for fructose formation increased as methanol<THF<GVL.

Keywords

Sn-SBA-15, Lewis acid catalyst, glucose isomerization, biomass conversion

1. Introduction

Lignocellulosic biomass appears as a reliable renewable source of carbon to produce chemicals and fuels [1]. Its structure is composed mainly by 40-50 % of cellulose (a polymer of glucose), 25-35 % of hemicellulose (polymer of mainly xylose), and 15-20 % of lignin [1]. The chemical conversion of cellulose, the major component of lignocellulosic biomass, can lead to the formation of 5-hydroxymethylfurfural (HMF), a platform molecule for producing chemical intermediates, fuels and monomers for plastics [1]. Indeed, HMF has been listed among the most important bio-based chemicals obtained from carbohydrates [2,3].

Glucose can be converted to HMF with high selectivity using a combination of Lewis and Brønsted acids [4–7]. The former is responsible for isomerizing glucose to fructose, which is subsequently dehydrated by the Brønsted acid [4–6]. Combinations of HCl or Amberlyst acid resin with Lewis acids such as metal chlorides [4] or Sn-Beta Zeolite [5,6,8,9] displayed good performance for HMF production.

Indeed, Sn-Beta Zeolite gained popularity in the last years as a water compatible solid Lewis acid catalyst for isomerization [8], retro aldol-condensation [10], and Diels-Alder reaction [11]. In the case of glucose isomerization, two different Sn sites have been identified: (i) the close sites, in which Sn is tetrahedrically coordinated with the silica framework [$Sn(OSi)_4$]; (ii) the open sites, formed by the hydrolysis of one bond in the close sites [$Sn(OSi)_3(OH)$] [8]. The open sites will also have a vicinal silanol group [$(OSi)_3Si\text{-}OH$] formed in the hydrolysis. Mechanistic studies indicated that the open sites are responsible for the isomerization of glucose to fructose, and the coordination of glucose takes place in both Sn and the vicinal Si-OH sites [12,13]. Hence, for the Sn site

to be active for fructose formation, a vicinal silanol is necessary. In the absence of silanol, the catalyst promotes the epimerization of glucose to mannose [12].

The importance of silanol in the proximity of the Sn sites must be taken in consideration aiming to improve the catalyst performance. Zeolites, due to its crystalline nature, have a low concentration of silanol groups and therefore, the Sn needs to be open to provide the vicinal silanol. On the other side, amorphous silica has high concentration of surface silanols and therefore would be an ideal scaffold for Sn. In this case, Sn would be surrounded by Si-OH no matter if the site is open or closed. Another important consideration is that Beta Zeolite has micropores with diameter smaller than the size of glucose (0.86 nm) [14]. Previous works suggest that for an efficient diffusion of glucose in the catalyst structure, pores need to be of at least 0.9 nm [15,16].

Therefore, for glucose isomerization to fructose an ideal Lewis acid catalyst based on Sn-silica must contain Sn ions coordinated to the silica framework, high silanol content, and large pore sizes. In this context, Sn containing mesoporous silica SBA-15 appears to be a promising candidate for glucose isomerization, since it typically presents high silanol density (>3 OH nm^{-2}) [17], surface area (> 600 m^2 g^{-1}) [18], and pore size (> 6 nm) [18].

This contribution thus aims at engineering a Sn-SBA-15 catalyst for glucose isomerization. The effect of the SBA-15 synthesis pH and Sn loading in the Sn-SBA-15 structure, porosity, and type of generated Sn species on catalyst activity towards glucose isomerization is systematically evaluated.

2. Materials and methods

2.1. Synthesis of Sn-SBA-15

Sn-SBA-15 was synthesized in a polypropylene beaker, dissolving 4g of Pluronic P123 (Sigma-Aldrich) in 100 g of a hydrochloric acid aqueous solution (0.028, 0.049 or 0.070 mol L^{-1}). The solution was heated up to 40 °C in an oil bath and 9.0 g of tetraethylorthosilicate (TEOS, 98 %, Sigma-Aldrich) were added followed by 0.227, 0.454 or 0.682 g of tin(IV) chloride pentahydrate ($SnCl_4.5H_2O$, 98 %, Sigma-Aldrich) to yield a nominal mol % of Sn of 1.5, 3.0, and 4.5 mol %, respectively. The reaction was stirred under the same temperature for 24 h and aged in autoclave for another 24 h at 100 °C. The white solid was filtered, washed thoroughly with distillated water, dried on air for 24 h, and calcined for 5 h at 550 °C (1 °C min^{-1}).

The samples were named based on the synthesis parameters, as shown in **Table 1**.

Table 1. Synthesis parameters, labels of the Sn-SBA-15 samples and determination of Sn loading by ICP-OES.

Sample name	HCl concentration (mol L^{-1})	Theoretical Sn mol %	Measured Sn mol %
Sn-SBA-15-0.028M-3.2%	0.028	3.0	3.2
Sn-SBA-15-0.07M-2.5%	0.07	3.0	2.5
Sn-SBA-15-0.049M-1.4%	0.049	1.5	1.4
Sn-SBA-15-0.049M-2.5%	0.049	3.0	2.5
Sn-SBA-15-0.049M-4.5%(3.0%)*	0.049	4.5	3.0

*This sample was named with both theoretical and measured Sn loading due to the large difference between them.

2.2. Mesoporous catalysts characterization

X-ray diffractograms were collected in a Bruker D8 Advance with DaVinci design diffractometer with a Lynxeye position sensitive detector. UV-Vis spectra were obtained in a Shimadzu UV 3600 spectrometer, using $BaSO_4$ as blank. Nitrogen physisorption isotherms at -196 °C were obtained in a Micromeritics ASAP 2420. Surface area was calculated from the isotherm using the BET (Brunauer, Emmet e Teller) equation in the range between of relative pressure within 0.02 to 0.2. The pore size distribution was calculated from the desorption branch using NLDFT method for silica with cylindrical pores. Microporous area was calculated using t-plot with the aid of the Micromeritics software assistant, using data points in the relative pressure range between 0.3 and 0.5. The size of silica wall between the pores were calculated by subtracting the pore size from the size of the unit cell obtained from X-ray diffraction. Sn loading was determined by inductively coupled plasma optical emission spectroscopy (ICP-OES) in a Varian Vista MXP spectrometer. Samples were firstly calcined at 900 °C for 6 h (5 °C min^{-1}), then dissolved in a mixture of HNO_3 and HF in a DGT 100 Plus Digester (Provecto Analítica). A selected catalyst was characterized by TPD-NH_3 with a multipurpose homemade apparatus equipped with a Pfeiffer QME 200 mass spectrometer to quantify the loading of Lewis acidity. Approximately 0.1 g of sample was pretreated at 150 °C under He flow (60 mL min^{-1}) for 2 h. Sequentially, the system temperature was dropped to 100 °C and a mixture of 4 vol. % NH_3/He was admitted (60 mL min^{-1}) for 1 h. Then, the system was purged with He (60 mL min^{-1}) for 1 h and then heated to 800 °C (10 °C min^{-1}) still under flow of He.

2.3. Catalytic activity

Catalytic studies were performed in 9 mL thick glass reactors at 110 °C. In typical runs, the reactions were loaded with 0.025 g of Sn-SBA-15 and 5 mL of a 1 wt. % glucose solution in different organic solvents [methanol, γ-valerolactone (GVL), or tetrahydrofuran (THF)] containing 20 wt. % of water (corresponding to an organic solvent/water weight ratio of 4/1). The reactions were terminated by cooling down the glass reactor in ice bath. Dimethylsulfoxide was used as internal standard in all reactions.

Direct conversion of glucose to 5-hydroxymethylfurfural was performed similarly to the methodology described above but adding HCl to a concentration of 0.2 mol L^{-1}.

The reaction mixtures were quantified by high-performance liquid chromatography (HPLC) in a Shimadzu LC-10/20 chromatograph equipped with a Bio-Rad Aminex HPX-87H (300x7.8 mm) at 65 °C using 0.005 mol L^{-1} H_2SO_4 as mobile phase. Quantification of glucose, fructose, and 5-hydroxymethylfurufral (HMF) were performed using calibration curves built with commercial standard chemicals. HMF was analyzed with a diode array detector at 254 nm and the monosaccharides using a refraction index detector at 40 °C.

Average turnover number (TON) reported in **Figure 5** was calculated using the concentration of molar amount of fructose at 150 min of reaction. Average TON was calculated using the equation below:

$$TON = \frac{(mol\ fructose\ formed)}{(catalyst\ weight)x(mol\ Sn\ per\ gram\ of\ catalyst)x(reaction\ time)}$$

Initial turnover frequency (TOF) reported in **Figure 6** was obtained as the linear coefficient of the graph "TOF as a function of reaction time" (**SI**). TOF for each reaction time was calculated using the amount of acid sites obtained by NH_3-TPD (0.311 mmol g^{-1}, as shown in **SI**) and the equation below.

$$TOF = \frac{(mol\ fructose\ formed)}{(catalyst\ weight)x(mol\ of\ acid\ sites\ from\ NH3-TPD)x(time)}$$

3. Results and discussion

The quantification of the Sn loading in the SBA-15 samples was carried out by inductively coupled plasma optical emission spectroscopy (ICP-OES) and the results are displayed in **Table 1**. For the samples prepared nominally with the lowest Sn loading and the one prepared with the lowest acid concentration, the measured and nominal Sn loading presented small deviation (7 %). The other samples prepared with 3 % of Sn reached a measured loading of 2.5 %, a deviation of 14 %. Only 3 % of Sn was incorporated in the sample prepared with 4.5 %. Surprisingly, although the Sn was not fully incorporated, its higher loading in the solution was enough to affect the structural properties of the sample, as discussed below. As shown in **Table 1,** the samples were named after the HCl concentration in the synthesis gel and the measured Sn loading, except for Sn-SBA-15-0.049M-4.5%(3.0%), in which both theoretical and measured Sn loadings are described to avoid misunderstanding with samples prepared with 3 % of Sn in the synthesis gel.

X-ray diffraction (XRD) was used to evaluate how the SBA-15 structure is affected by the concentration of acid (0.028, 0.049, or 0.07 mol L^{-1}) and of the Sn precursor (1.5, 3.0, and 4.5 mol % based on the silica source) in the synthesis gel. Typical XRD pattern for SBA-15 presents three peaks due to the planes assigned to the Miller indexes (100), (110) and (200), with ratios $2\theta_{(110)}/2\theta_{(100)} = \sqrt{3}$ and $2\theta_{(200)}/2\theta_{(100)} = 2$ [19]. The XRD patterns of the Sn-SBA-15 prepared varying the concentration of acid and the Sn loading are shown in **Figure 1.**

Varying the acid concentration and maintaining the Sn loading at 3 mol %, it was observed that the XRD of the material synthesized with the highest HCl concentration (Sn-SBA-15-0.07M-2.5%) presented two intense XRD peaks at 2θ of 0.77 ° and 0.89 °. In this range of 2θ only one peak due to the (100) plane is expected, hence, it appears that the sample has a bimodal distribution of the unit cell sizes, which are named in **Figure 1** as (100) and (100)'. Other three XRD peaks are observed for this sample (diffractogram multiplied by 5 times), the first at 2θ = 1.32 can be assigned to (110)', since its ratio with the position of (100)' is ca. √3. The second peak at 2θ = 1.52 is a mixture of the (200)' and (110), once its ratio with the position of (100)' is ca. 2 and with the position of (100) is ca. √3. The last peak, at 2θ = 1.78 is due to the plane (200).

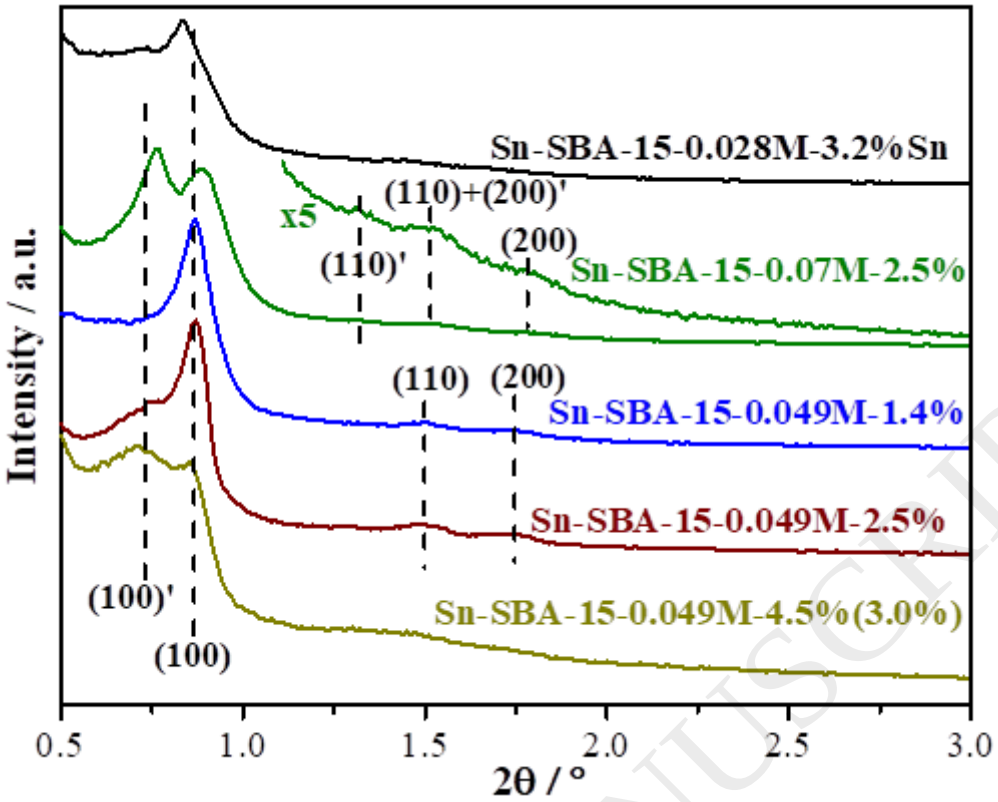

Figure 1. XRD diffraction patterns of Sn-SBA-15 synthesized varying the concentration of acid and the Sn loading.

The samples prepared with lower acid concentrations, Sn-SBA-15-0.028M-3.2% and Sn-SBA-15-0.049M-2.5%, have predominantly one unit cell size, whereas a slight contribution of a second unit cell parameter is present. Indeed, in this case a weak peak of the (100)' is observed while the peaks assigned to (110)' and (200)'are not. Sn-SBA-15-0.028M-3.2% did not present the peaks due to the Miller indexes (110) and (200), indicating a poor organization of the pores at long range. On the other hand, Sn-SBA-15-0.049M-2.5% displayed well resolved peaks due to the planes assigned to the Miller indexes (100), (110) and (200), indicating a well-organized SBA-15 structure.

Among the Sn-SBA-15 prepared with different HCl concentrations, Sn-SBA-15-0.049M-2.5%Sn is, by far, the one with better structural organization, since it presents low contribution of bimodal distribution of the unit cell and pores well-organized in a hexagonal array. Hence, the HCl concentration of 0.049 mol L^{-1} was chosen to prepare Sn-SBA-15 with different Sn loading (1.5 and 4.5 mol %).

As shown in **Figure 1**, increasing the Sn loading in the synthesis gel from 3 to 4.5 mol %, favored the bimodal distribution of the unit cell parameter and also reduced the

organization of the pores at higher-range, since the XRD peaks due to the planes (110) and (200) are not well defined. It is indeed surprising that according to ICP-OES only 3 % of Sn was incorporated in the structure, hence, increase of Sn concentration in solution was enough to change the structuration of the silica. Reducing the Sn loading to 1.5 mol % in the synthesis gel led to the formation of a well-defined Sn-SBA-15 with purely monomodal distribution of the unit cell parameter. From the XRD analyses, it can be concluded that both HCl concentration and Sn loading affect the structuration of SBA-15, at high concentration of acid or high Sn loading, bimodal distribution of the unit cell is promoted.

Table 2. Unit cell parameter (a_0), wall thickness (W), textural properties, and TOF for fructose formation for the Sn-SBA-15 prepared by different methods.[a]

Sample	a_0[b] / nm	S_{BET} / $m^2\ g^{-1}$	Dp / nm	Vp / $cm^3\ g^{-1}$	S_{micro} / $m^2\ g^{-1}$	Vp_{Micro} / $cm^3\ g^{-1}$	W[b] / nm	TOF / h^{-1}
Sn-SBA-15-0.028M-3.2%	12.1	875	8.6	1.03	216	0.09	3.5	0.31
Sn-SBA-15-0.07M-2.5%	13.2 / 11.5	885	7.2	0.90	268	0.11	6.0 / 4.5	0.24
Sn-SBA-15-0.049M-1.4%	11.7	900	8.1	0.90	261	0.11	3.4	0.24
Sn-SBA-15-0.049M-2.5%	11.7	901	8.3	1.06	243	0.10	3.4	0.33
Sn-SBA-15-0.049M-4.5%(3.0%)	14.4 / 12.0	885	8.6	0.90	207	0.09	5.8 / 3.4	0.13

[a] S_{BET} = specific surface area calculated by the BET method using the Rouquerol criteria; Dp = pore diameter; Vp = pore volume calculated at 0.90 (PP_0^{-1}); Smicro = microporous surface area; a_0 = unit cell parameter; W= wall thickness.

[b] In the case of bimodal distribution of the unit cell, both are reported separated by "/". Similarly, wall thickness was calculated for both.

While the ICP-OES analyses confirmed the presence of Sn in the Sn-SBA-15 prepared by different methods, it does not give evidences about the nature of the species formed, hence, diffuse reflectance UV–Visible spectroscopy was used to identify the Sn species (**Figure 2**). Typically, a band at 210 nm suggests Sn(IV) tetrahedrally-coordinated to the silica framework [20]. When these framework sites are hydrated with

one or two water molecules, the penta- and hexa-coordinated Sn species yield bands at 220 and 250 nm, respectively [20]. These three species have Lewis acidity [20]. Undesirable extraframework SnO_2 is identified to a band at 280 nm, and is not active as Lewis acid [21].

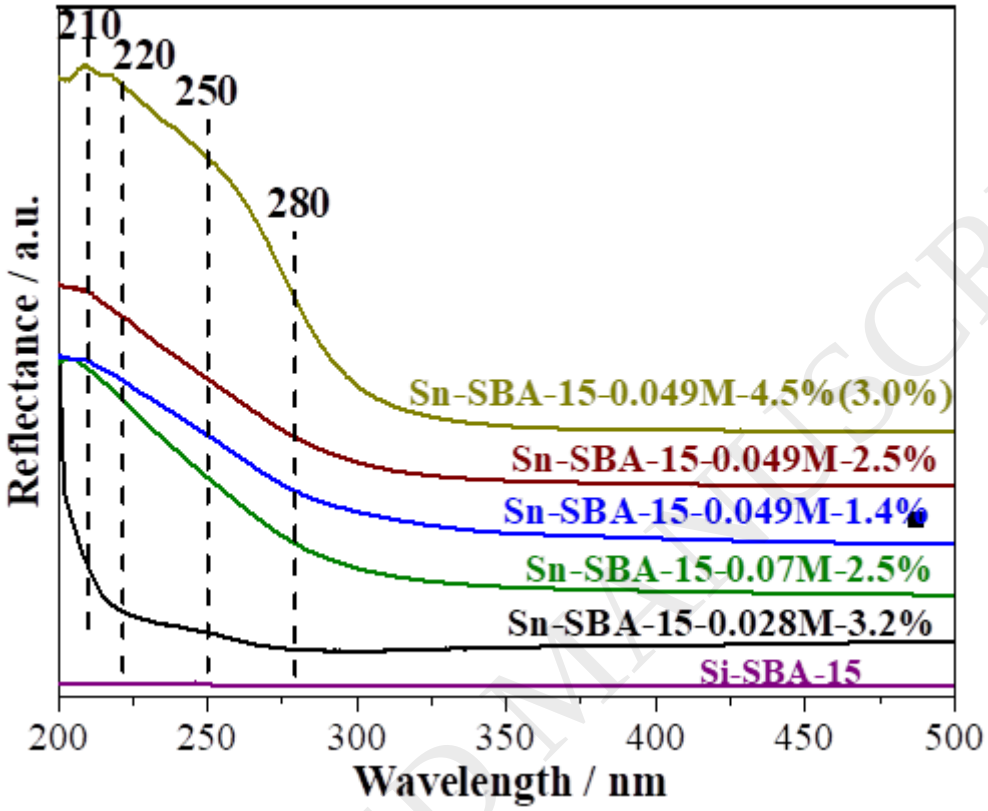

Figure 2. Diffuse reflectance UV–Visible spectra of Sn-SBA-15 prepared varying the concentration of acid and the Sn loading.

Sn-SBA-15-0.028M-3.2% presented a reflectance band 210 nm, indicating the preferential formation of tetrahedral Sn species, as previously observed for Sn-Beta Zeolite (**Figure 2**) [22]. As for the other samples, the spectra display a broad reflectance band due to tetrahedral Sn coordinated to the silica framework (210 nm) and its hydrated forms (220 and 250 nm). Extraframework SnO_2 was only observed for the sample with the highest Sn loading in the synthesis gel (Sn-SBA-15-0.049M-4.5%(3.0%)). Hence, for samples with up to 3 mol % of Sn in the synthesis gel, UV-Vis analyses confirmed that the heteroatom was fully introduced in the silica framework being present predominantly in the tetrahedral site or its hydrated form (penta- or hexa-coordinated), which are all Lewis acid centers.

The textural properties of the Sn-SBA-15 were studied by nitrogen physisorption at -196 °C (**Table 2**). For all samples, the adsorption branch of the isotherms presented three adsorption phenomena: (i) at $P/P_0 < 0.1$, the micropores are filled and a nitrogen monolayer is formed in the solid surface; (ii) at $0.6 < P/P_0 < 0.8$, the mesopores are filled by capillary condensation; and (iii) at $P/P_0 > 0.95$, non-structural pores formed in the interstices of the particles are filled with nitrogen. The samples displayed Type-IVa isotherms, typical for mesoporous molecular sieves [23]. In the desorption branch, a H1 hysteresis loop was observed, indicating well-defined cylindrical pores [23].

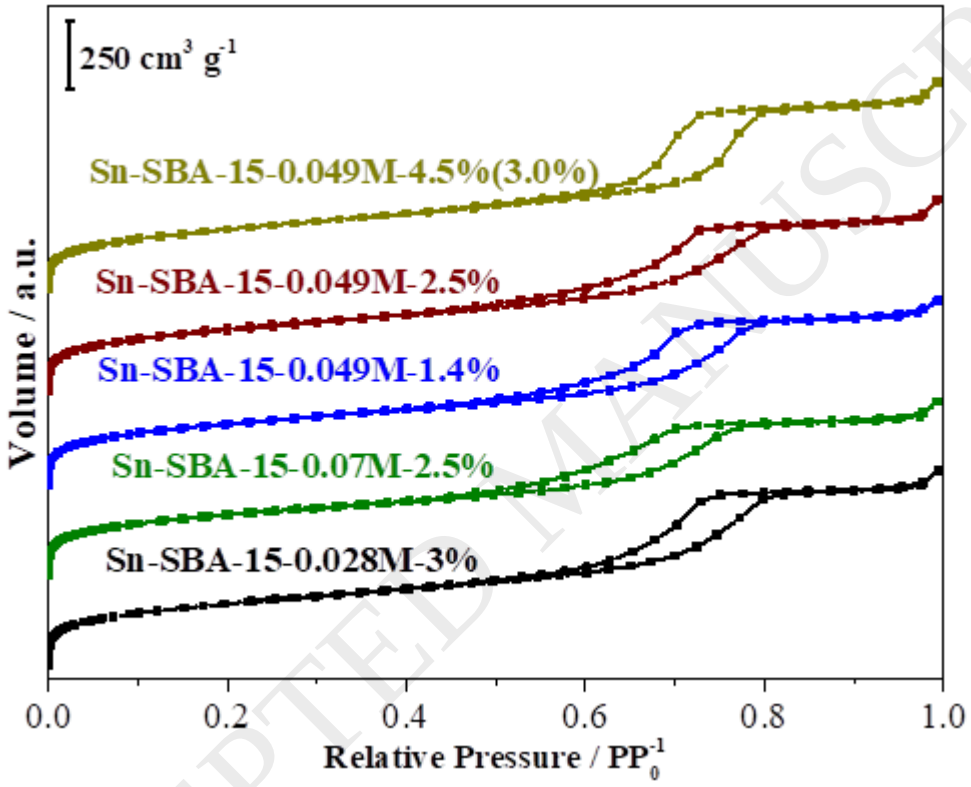

Figure 3. N_2 physisorption at -196 °C isotherms of Sn-SBA-15 prepared varying the concentration of acid and the Sn loading.

Specific surface areas (S_{BET}) (**Table 2**) ranged between 875 and 901 $m^2 g^{-1}$, and since the differences were within the analysis error (5 %), it can be concluded that S_{BET} was not significantly affected by the changes in the SBA-15 synthesis parameters.

The pore size distribution (**Figure 4**) reveals two families of pores: (i) the large mesopores (>4.5 nm), which are predominant in the SBA-15 structure; and (ii) the small mesopores and large micropores (1-4 nm), which are responsible for connecting the large mesopores. As it regards the later family of pores, they are similar for all samples. The

large micropores have indeed, a significant contribution in the materials prepared and account for a surface area (S_{micro}) of over 200 m^2 g^{-1} as well as the microporous volume (V_{micro}) is responsible for 10-12 % of the total pore volume (**Table 2**). Indeed, the presence of a well-defined microporosity is an indicative that SBA-15 structure was well formed.

As it regards the large mesopores, they were significantly affected by the variation of the Sn-SBA-15 synthesis parameters (**Figure 4**). For instance, only Sn-SBA-15-0.049M-2.5% and Sn-SBA-15-0.049M-4.5%(3.0%) displayed narrow and well-defined distribution of mesopores. This result is unexpected for Sn-SBA-15-0.049M-4.5%(3.0%), since its XRD (**Figure 1**) suggested an accentuated bimodal distribution of the unit cell parameter. Sn-SBA-15-0.07M-2.5%, which also had bimodal distribution of the unit cell (**Figure 1**), displayed the broadest distribution of the pore sizes, ranging from 4.5 to 10 nm. Interestingly, although Sn-SBA-15-0.049M-1.4% presents a single and well-defined unit cell parameter, its pore size distribution is as broad as the one observed for Sn-SBA-15-0.07M-2.5%. The average sizes of the large mesopores are given in **Table 2,** and they are indeed similar (8.3-8.6 nm) for all samples except for the Sn-SBA-15-0.07M-2.5% (7.2 nm) and Sn-SBA-15-0.049M-1.4% (8.1).

The unit cell length (a_0) and the average pore size (Dp) were used to estimate the thickness (W) of the silica wall between the pores ($W = a_0 - Dp$), as shown in **Table 2**. Except for Sn-SBA-15-0.07M-2.5%, the materials presented W of 3.4-3.5 nm. Sn-SBA-15-0.07M-2.5% and Sn-SBA-15-0.049M-4.5%(3.0%), the samples with bimodal distribution of a_0, also displayed an additional contribution of W between 5.8 and 6.0 nm. These results indicate the formation of mesoporous silica with considerable thick walls, which confers good stability.

Altogether these results show that different Sn-SBA-15 materials were indeed synthesized by modifying preparation conditions. Distinct pore size distribution while keeping essentially the same overall surface area and the generation of different Sn species can be highlighted as some of the tailored properties that may strike catalytic activity.

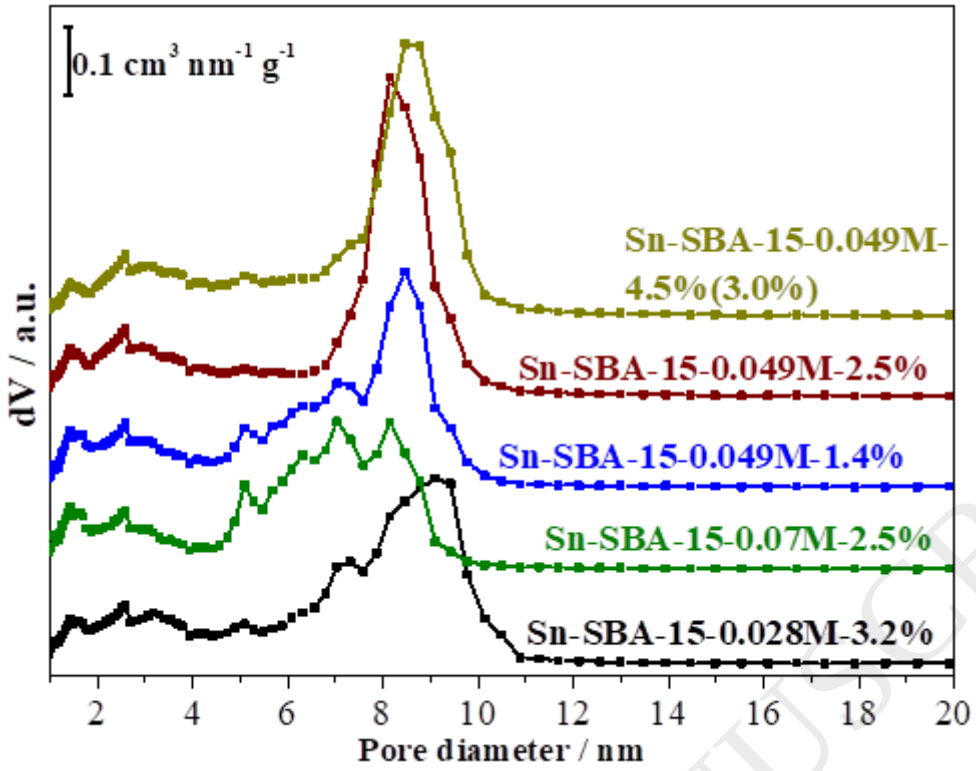

Figure 4. Pore size distribution calculated by DFT from N_2 isotherms.

These tailored Sn-SBA-15 solids were firstly tested in the isomerization of glucose to fructose at 110 °C, using methanol containing 20 wt. % of water (methanol/water weight ratio of 4/1) as solvent. The use of water as co-solvent has been showed before to be beneficial for monosaccharides conversion [5,24,25]. Reaction data after 150 min are depicted in **Figure 5**. The equilibrium constant for the reaction is close to the unit, hence, to warranty studies under kinetic regime, reactions were performed at conversions below 20 %. The samples prepared with 3 mol % of Sn led to similar selectivities to fructose (83.4 to 84.5 %). However, Sn-SBA-15-0.028M-3.2% and Sn-SBA-15-0.049M-2.5% displayed the highest conversions (11.9 and 11.8 %) while the reaction carried out over Sn-SBA-15-0.07M-2.5% reached only 8.2 %. The difference in conversion might be associated to the catalyst pore size, since Sn-SBA-15-0.07M-2.5% has the smallest pores (7.2 nm, **Table 2**) among all samples. It could entail in a slower diffusion of the monosaccharides through the pores.

Sn-SBA-15-0.049M-1.4% and Sn-SBA-15-0.049M-4.5%(3.0%) reached similar glucose conversion (8.2 and 7.7 %) and fructose selectivities (76.0 and 74.0 %), which are lower than the ones found for the samples prepared with 3.0 mol % of Sn. Indeed, Sn-SBA-15-0.049M-4.5%(3.0%) displayed the lowest conversion and selectivity among all

catalysts. This finding may be ascribed to the high contribution of extraframework SnO_2 species formed in this catalyst, as observed by UV-Vis (**Figure 2**). SnO_2 has been reported to be inactive in glucose isomerization [26] but able to degrade fructose [27]. Indeed, the poor performance of Sn-SBA-15-0.049M-4.5%(3.0%) is endorsed by its average turnover number (average TON) for fructose formation, which was found to be ca. 2.4 and 2.6 times lower than the ones found for Sn-SBA-15-0.028M-3.2% and Sn-SBA-15-0.049M-2.5%, respectively (**Figure 5**). Sn-SBA-15-0.049M-1.4%Sn and Sn-SBA-15-0.07M-2.5%, the two samples with broad pore size distribution (**Figure 4**), achieved similar average TON, endorsing that the diffusion of the monosaccharides is indeed limiting the activity.

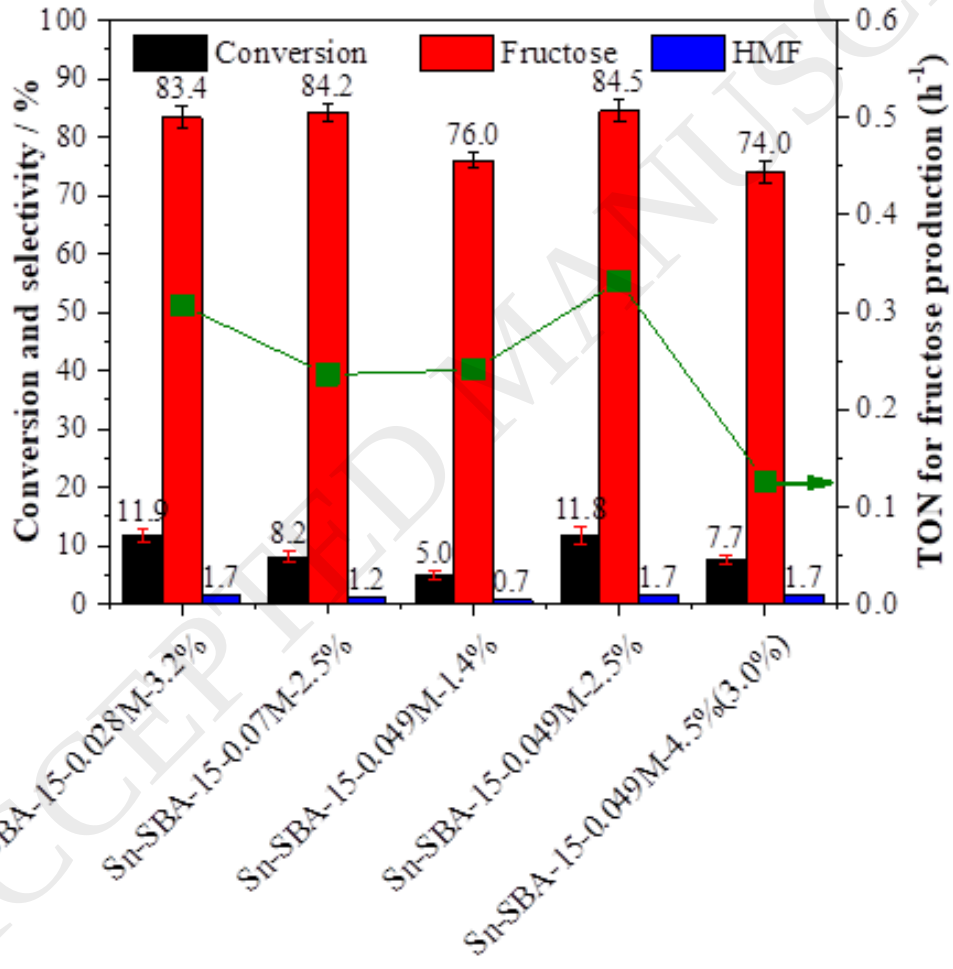

Figure 5. Conversion of glucose, selectivity to fructose and HMF, and average TON for fructose formation. Reaction conditions: 1 wt. % glucose in methanol/H_2O (4/1 wt. ratio), 110 °C, and 150 min of reaction.

Based on the characterization and these preliminary catalytic tests, it can be seen that Sn-SBA-15-0.049M-2.5% displays the best compromise between activity and structural properties: (i) well-defined SBA-15 structure, although a slight contribution of a second unit cell parameter was observed by XRD; (ii) the highest surface area (901 m^2 g^{-1}) and pore volume (1.06 cm^3 g^{-1}); (iii) narrowest pore size distribution, with an average at 8.3 nm; and (iv) highest glucose consumption, fructose selectivity and TOF. In order to rule out the possibility of leaching of Sn in this sample, it was analyzed by ICP-OES before and after reaction (**SI**). No significant change was observed, indicating that the Sn sites are not significantly affected by the reaction conditions. Hence, the catalytic properties of Sn-SBA-15-0.049M-2.5% were studied further in different solvents.

Kinetic studies for glucose conversion were performed in different organic solvents [methanol, tetrahydrofuran (THF), and γ-valerolactone (GVL)] containing 20 wt. % of water. Indeed, the nature of the solvent has been shown to play an important role in the kinetic and mechanism of biomass-derived monosaccharides [1,5,25,28–34]. As mentioned before, in order to obtain reliable kinetic data under the kinetic regime, avoiding mass transfer issues, reaction data were collected at conversions below 20 %.

In the three solvent systems investigated, conversion of glucose increases along with time (**Figure 6**). Methanol and THF follow a similar trend of conversion, while GVL leads to higher conversion. As for the fructose selectivity, time-dependent trends disclose different patterns despite reaching similar values at 150 min independent of the solvent system. By using methanol, selectivity to fructose increases with conversion, reaching ca. 85 % at 150 min reaction. In contrast, it is seen to steadily decrease from 97 to 85% when GVL is used while it is pretty much not disturbed in THF, holding 85% within the whole studied time interval. Reactions were also performed at high conversion (ca. 40 %) for all solvent systems and are reported in **SI**. For the sake of comparison, the catalytic performance for Sn-SBA-15-0.049M-2.5% were also compared with the one for Sn-MCM-41-3% (**SI**).

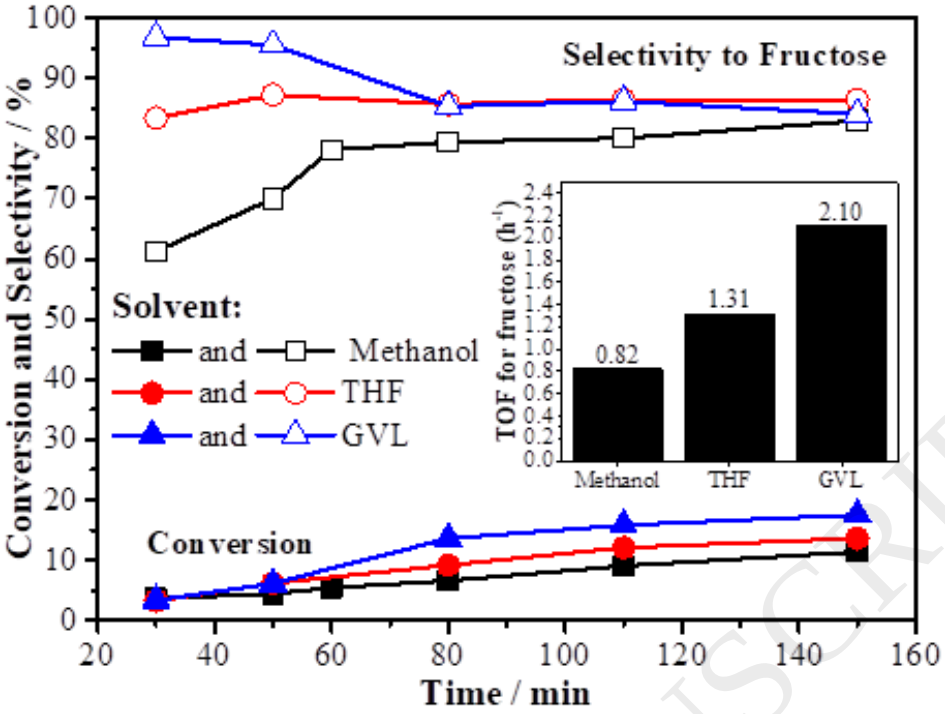

Figure 6. Conversion of glucose and selectivity to fructose as a function of time for reactions carried out in methanol, THF or GVL containing 20 wt. % of water as solvent at 110 °C. INSET: Initial TOF for fructose formation in the different solvent systems.

The initial TOF for fructose formation was significantly affected by the solvent system used (**Figure 6-inset** and **SI**). In the reaction carried out in GVL/H_2O = 4/1, the initial TOF was 2.10 h^{-1}, 2.6 and 1.6 times higher than the ones obtained for methanol/H_2O and THF/H_2O, respectively. Indeed, the solvent used can affect the reaction mechanism and/or the energy of the transition state states [32,35,36]. It has been shown that the extent of solvation directly affects the initial and transition states in the catalytic process of monosaccharides conversion, controlling the reaction rate and the product selectivity [32,35]. Furthermore, the solvent can also affect the energy of the free energy of the active site species [32,35].

In the isomerization of glucose to fructose catalyzed by Sn-silicates, small fractions of water in the organic solvent affect the activity and stability of the active site as the presence of water is important to guarantee the hydration of the Sn sites, preserving its activity towards glucose isomerization [36]. It has been found that in [organic solvent]/water solvent systems, the availability of water to react depends on the enthalpies of mixing (ΔH^M) between water and the organic solvent, i.e., the reactivity increases with

the endothermicity of the ΔH^M. According to the literature, the approximate values of ΔH^M for a mixture of methanol, THF, or GVL with 20 wt. % of water are -0.58, -0.20, and +0.65 kJ mol^{-1} [35,37] and, indeed, the TOF (**Figure 6-inset)** increases along with the ΔH^M in a linear trend (**SI**).

Due to the promising performance of Sn-SBA-15-0.049M-2.5%, it was also tested in the direct conversion of glucose to 5-hydroxymethylfurfural (HMF). In this case, the Lewis catalyst needs to be combined with a Brønsted acid catalyst, which is responsible for dehydrating the fructose formed into HMF. Although GVL was shown to be the best solvent for glucose isomerization, previous work has shown that for the direct conversion of glucose to HMF, THF leads to higher selectivities [33]. Therefore, using THF/H_2O = 4/1 as solvent, Sn-SBA-15-0.049M-2.5% was combined with HCl (0.2 mol L^{-1}) as Brønsted acid catalyst. Studies were performed at high conversion to allow comparison with results in literature that also used HCl as Brønsted acid. As shown in **Table 3**, the combination of Sn-SBA-15-0.049M-2.5% and HCl leads to a HMF yield of 57 %, similar to the results obtained before using a combination of Sn-Beta zeolite and HCl [6]. By using a combination of two homogeneous catalysts ($AlCl_3$/HCl), slightly higher yields of 61 % were achieved [33]. It is important to mention that Sn-SBA-15-0.049M-2.5% presented promising results not only for fructose production, but when combined with a Brønsted acid, it can also produce HMF with high yields.

Table 3. One-pot conversion of glucose in HMF using HCl as Brønsted acid and different Lewis acids.

Lewis Acid	**Brønsted Acid**	**Conversion / %**	**Selectivity to HMF / %**	**Yield / %**	**Ref**
Sn-SBA-15-0.049M-2.5%	HCl (0.2 mol L^{-1})	97	59	57	This work
Sn-Beta	HCl (0.1 mol L^{-1})	79	72	57	[6]
$AlCl_3$	HCl (0.014 mol L^{-1})	90	56	61	[33]

4. Conclusion

The concentration of HCl (0.028, 0.049, and 0.07 mol L^{-1}) and the Sn loading (1.5, 3.0, and 4.5 mol %) showed to significantly affect the structural and textural properties of Sn-SBA-15, impacting their catalytic activity. Increasing the acid concentration and the Sn loading led to a bimodal distribution of the unit cell parameter and it was found that, as structure is concerned, the best synthesis conditions is 0.049 mol L^{-1} of HCl and Sn loading between 1.5 and 3.0 %.

Analysis of the Sn species showed that tetrahedral tin coordinated to the silica framework and its hydrated form are predominant in all samples. The sample prepared with the highest Sn loading (4.5 %) had an important contribution of extraframework SnO_2, which has been shown before not to be active in the reaction studied in this work. Hence, it is clear that the synthesis method applied in this work is limited to a maximum of 3 mol % of tin to warranty complete insertion of the heteroatoms in the silica net.

Surface area, pore volume, and microporosity formation was not significantly affected by the synthesis parameter, while the distribution of the large mesopores was. Samples prepared with lowest Sn loading (1.5 %) and the highest acid concentration (0.07 mol L^{-1}) displayed the broadest pore size distribution. Surprisingly, there was no direct correlation between bimodal distribution of the unit cell and broad distribution of the mesopores.

Indeed, the catalysts with broad size distribution presented lower TOF for fructose formation compared to the ones with narrow distribution. The highest TOF was achieved for the sample prepared with 3 mol % of Sn and acid concentration of 0.049 mol L^{-1} (Sn-SBA-15-0.049M-2.5%). The sample with the highest Sn loading and with contribution of SnO_2 reached the lowest TOF for fructose formation.

It was found that Sn-SBA-15-0.049M-2.5% rendered the more suitable catalyst, displaying the best compromise between activity and structural properties: (i) well-defined SBA-15 structure; (ii) the highest surface area and pore volume; (iii) narrowest pore size distribution; and (iv) highest glucose conversion, fructose selectivity and TON.

The catalytic activity of this sample was also studied in methanol, tetrahydrofuran (THF) and γ-valerolactone (GVL), all containing 20 wt. % of water, and the initial TOF for fructose formation increased as methanol<THF<GVL.

Sn-SBA-15-0.049M-2.5% combined with HCl formed an efficient catalytic system for the production of HMF in high yields (57 %) directly from glucose. These results are comparable with other catalytic systems previously reported in the literature.

5. References

[1] J.M.R. Gallo, M.A. Trapp, J. Braz. Chem. Soc. 28 (2017) 1586–1607.

[2] J.J. Bozell, G.R. Petersen, Green Chem. 12 (2010) 539.

[3] J.E. Holladay, J.F. White, J.J. Bozell, D. Johnson, Top Value-Added Chemicals from Biomass, Volume II - Results of Sreening for Potential Candidates from Biorefinery Lignin, 2007.

[4] Y.J. Pagán-Torres, T. Wang, J.M.R. Gallo, B.H. Shanks, J.A. Dumesic, ACS Catal. 2 (2012).

[5] J.M.R. Gallo, D.M. Alonso, M.A. Mellmer, J.A. Dumesic, Green Chem. 15 (2013) 85.

[6] E. Nikolla, Y. Román-Leshkov, M. Moliner, M.E. Davis, ACS Catal. 1 (2011) 408–410.

[7] A. Mithöfer, W. Plass, J.M.R. Gallo, J.L. Vieira, M. Almeida-Trapp, Catal. Today (2018).

[8] R. Bermejo-Deval, R.S. Assary, E. Nikolla, M. Moliner, Y. Roman-Leshkov, S.-J. Hwang, A. Palsdottir, D. Silverman, R.F. Lobo, L.A. Curtiss, M.E. Davis, Proc. Natl. Acad. Sci. 109 (2012) 9727–9732.

[9] Y. Román-Leshkov, M.E. Davis, ACS Catal. 1 (2011) 1566–1580.

[10] M.E. Davis, Top. Catal. 58 (2015) 405–409.

[11] J.J. Pacheco, M.E. Davis, Proc. Natl. Acad. Sci. 111 (2014) 8363–8367.

[12] R. Bermejo-Deval, M. Orazov, R. Gounder, S.J. Hwang, M.E. Davis, ACS Catal. 4 (2014) 2288–2297.

[13] N. Rai, S. Caratzoulas, D.G. Vlachos, ACS Catal. 3 (2013) 2294–2298.

[14] A. Corma, From Microporous to Mesoporous Molecular Sieve Materials and Their Use in Catalysis, 1997.

[15] K. Lourvanij, G.L. Rorrer, Dehydration of Glucose to Organic Acids in Microporous Pillared Clay Catalysts, 1994.

[16] J. Jae, G.A. Tompsett, A.J. Foster, K.D. Hammond, S.M. Auerbach, R.F. Lobo, G.W. Huber, J. Catal. 279 (2011) 257–268.

[17] L. Wang, R.T. Yang, J. Phys. Chem. C 115 (2011) 21264–21272.

[18] M. Kruk, M. Jaroniec, C.H. Ko, R. Ryoo, Chem. Mater. 12 (2000) 1961–1968.

[19] J.M.R. Gallo, C. Bisio, G. Gatti, L. Marchese, H.O. Pastore, Langmuir 26 (2010) 5791–800.

[20] N.K. Mal, A. V. Ramaswamy, Appl. Catal. A Gen. 143 (1996) 75–85.

[21] R. Bermejo-Deval, R. Gounder, M.E. Davis, ACS Catal. 2 (2012) 2705–2713.

[22] M. Moliner, Y. Roman-Leshkov, M.E. Davis, Y. Román-Leshkov, M.E. Davis, Proc. Natl. Acad. Sci. U. S. A. 107 (2010) 6164–6168.

[23] S. Lowell, J.E. Shields, M.A. Thomas, M. Thommes, Characterization of Porous Solids and Powders: Surface Area, Pore Size and Density, Springer Netherlands, Dordrecht, 2004.

[24] M.A. Mellmer, D. Martin Alonso, J.S. Luterbacher, J.M.R. Gallo, J.A. Dumesic, Green Chem. 16 (2014).

[25] E.I. Gurbuz, J.M.R. Gallo, D.M. Alonso, S.G. Wettstein, W.Y. Lim, J.A. Dumesic, E.I. Gürbüz, J.M.R. Gallo, D.M. Alonso, S.G. Wettstein, W.Y. Lim, J.A. Dumesic, Angew. Chemie. Int. Ed. English 52 (2013) 1270–1274.

[26] Y. Román-Leshkov, M. Moliner, J.A. Labinger, M.E. Davis, Angew. Chemie - Int. Ed. 49 (2010) 8954–8957.

[27] G. Raveendra, M. Surendar, P.S. Sai Prasad, New J. Chem. 41 (2017) 8520–8529.

[28] J.S. Luterbacher, J.M. Rand, D.M. Alonso, J. Han, J.T. Youngquist, C.T. Maravelias, B.F. Pfleger, J.A. Dumesic, Science (80-.). 343 (2014) 277–280.

[29] D.M. Alonso, S.G. Wettstein, J.A. Dumesic, Green Chem. 15 (2013) 584.

[30] M.H. Tucker, R. Alamillo, A.J. Crisci, G.M. Gonzalez, S.L. Scott, J.A. Dumesic, ACS Sustain. Chem. Eng. 1 (2013) 554–560.

[31] M.A. Mellmer, D. Martin Alonso, J.S. Luterbacher, J.M.R. Gallo, J.A. Dumesic, Green Chem. 16 (2014) 4659–4662.

[32] M.A. Mellmer, C. Sener, J.M.R. Gallo, J.S. Luterbacher, D.M. Alonso, J.A. Dumesic, Angew. Chemie - Int. Ed. 53 (2014) 11872–11875.

[33] J.A. Dumesic, J.M.R. Gallo, D. Alsonso, Method to Convert Monosaccharides to 5-(Hydroxymethyl) Furfural (HMF) Using Biomass-Derived Solvents, 2014.

[34] D.M. Alonso, J.M.R. Gallo, M.A. Mellmer, S.G. Wettstein, J.A. Dumesic, Catal. Sci. Technol. 3 (2013) 927–931.

[35] C. Sanpitakseree, P. Bai, J.A. Dumesic, K. Ma, M.A. Mellmer, M. Neurock, B. Demir, Nat. Catal. 1 (2018) 199–207.

[36] S. Saravanamurugan, M. Paniagua, J.A. Melero, A. Riisager, J. Am. Chem. Soc. 135 (2013) 5246–5249.

[37] R.F. Lama, B.C.Y. Lu, J. Chem. Eng. Data 10 (1965) 216–219.